remote sensing

MDPI

Letter

Retrieval of Aerosol Optical Depth Using the Empirical Orthogonal Functions (EOFs) Based on PARASOL Multi-Angle Intensity Data

Yang Zhang [1,2], Zhengqiang Li [1,*], Lili Qie [1], Weizhen Hou [1], Zhihong Liu [3], Ying Zhang [1], Yisong Xie [1], Xingfeng Chen [1] and Hua Xu [1]

1 Environment Protection Key Laboratory of Satellite Remote Sensing, Institute of Remote Sensing and Digital Earth, Chinese Academy of Sciences, Beijing 100101, China; zhangyang2015@radi.ac.cn (Y.Z.); qiell@radi.ac.cn (L.Q.); houwz1982@163.com (W.H.); zhangying02@radi.ac.cn (Y.Z.); xieys@radi.ac.cn (Y.X.); chenxf@radi.ac.cn (X.C.); xuhua@radi.ac.cn (H.X.)

2 University of Chinese Academy of Sciences, Beijing 100049, China

3 College of Resources and Environment, Chengdu University of Information Technology, Chengdu 610225, China; wxzlzh@cuit.edu.cn

* Correspondence: lizq@radi.ac.cn; Tel.: +86-10-6485-7437; Fax: +86-10-6480-6225

Academic Editor: Richard Müller
Received: 26 April 2017; Accepted: 7 June 2017; Published: 9 June 2017

Abstract: Aerosol optical depth (AOD) is a widely used aerosol optical parameter in atmospheric physics. To obtain this parameter precisely, many institutions plan to launch satellites with multi-angle measurement sensors, but one important step in aerosol retrieval, the estimation of surface reflectance, is still a pressing issue. This paper presents an AOD retrieval method based on the multi-angle intensity data from the Polarization and Anisotropy of Reflectances for Atmospheric Science coupled with Observations from a Lidar (PARASOL) platform using empirical orthogonal functions (EOFs), which can be universally applied to multi-angle observations. The function of EOFs in this study is to estimate surface intensity contributions, associated with aerosol lookup tables (LUTs), so that the retrieval of AOD can be implemented. A comparison of the retrieved AODs for the Beijing, Xianghe, Taihu, and Hongkong_PolyU sites with those from the Aerosol Robotic Network (AERONET) ground-based observations produced high correlation coefficients (r) of 0.892, 0.915, 0.831, and 0.897, respectively, while the corresponding root mean square errors (RMSEs) are 0.095, 0.093, 0.099, and 0.076, respectively.

Keywords: aerosol optical depth; retrieval; multi-angle remote sensing; empirical orthogonal functions; PARASOL; AERONET; East China; bright regions

1. Introduction

Aerosol optical depth (AOD) is an important aerosol optical parameter with many applications in the fields of atmospheric studies and climate change [1–7]. Recently, we proposed an aerosol fine-mode fraction (FMF) retrieval method [8] which uses the ratio of the fine-mode AOD (AOD_f) to the total AOD to obtain FMF. This method has been implemented on the Polarization and Anisotropy of Reflectances for Atmospheric Science coupled with Observations from a Lidar (PARASOL) platform, which has the ability to detect the intensity and polarization of radiation from multi-angle observations. However, one important part in our AOD retrieval process, the estimation of the surface intensity reflectance, has some defects. In the current approach, we use a semi-empirical model [9] to estimate the surface intensity reflectance. Although the model may help obtain comparable AOD retrievals from the Aerosol Robotic Network (AERONET) ground-based observations, the semi-empirical parameter used in that model varies with the study region, which limits the application scope of our FMF retrieval method. Moreover, many countries now plan to launch new satellites with multi-angle measurement

sensors for aerosol detection, but the estimation of the surface reflectance is always a difficult issue. Although the Moderate-resolution Imaging Spectroradiometer (MODIS) platform provides an efficient dark target (DT) algorithm to obtain the surface reflectance [10,11], the 2.1 μm channel is required for this method, and it cannot solve the problem of estimating the surface reflectance over bright regions. Therefore, we need a surface reflectance estimation method that can be widely used in multi-angle remote sensing and that is not affected by the surface type.

In the Multi-angle Imaging SpectroRadiometer (MISR) operational aerosol retrieval algorithm, a mathematical method, empirical orthogonal functions (EOFs), is used to obtain the surface contribution, which gives a general solution for the surface reflectance estimation in multi-angle aerosol remote sensing [12–14]. PARASOL is similar to MISR—it has the ability to detect an intensity signal from, at most, 16 angles, and EOFs could accordingly be applied to its observations. Therefore, this paper focuses on using the EOFs to obtain the surface intensity reflectance from the PARASOL multi-angle intensity observations, thereby providing another application of EOFs in addition to MISR. We chose East China as the study area. The introduction of EOFs for surface contribution estimation and AOD retrieval are presented in Section 2. The retrieval results using EOFs and the validations against the AERONET ground-based observations are presented in Section 3. A discussion of EOFs is given in Section 4. The last section presents the conclusions of the study.

2. Methodology

The flow chart for the retrieval of AOD is shown in Figure 1. The study is separated into three parts: the construction of the lookup tables (LUTs), data preprocessing, and the retrieval of AOD. For the derivation of LUTs, several aerosol models were input into the Second Simulation of a Satellite Signal in the Solar Spectrum, Vector version (6SV) radiative transfer code [15–17]. For the data preprocessing, the cloud mark was first extracted from the PARASOL Level 1 data to help recognize the cloud pixels; the cloudy pixels were not processed. The multi-angle intensity data were used to build the covariance matrix from which the EOFs can be calculated from; the EOFs were used to estimate the surface contribution. For the AOD retrieval, the LUTs and EOFs were used to simulate the reflectance at the top of atmosphere (TOA), and after a comparison between the simulated and observed TOA reflectance, the optimal aerosol model and AOD could finally be determined. The spatial resolution of the retrieved AOD is approximately 19 km (3 × 3 PARASOL pixels).

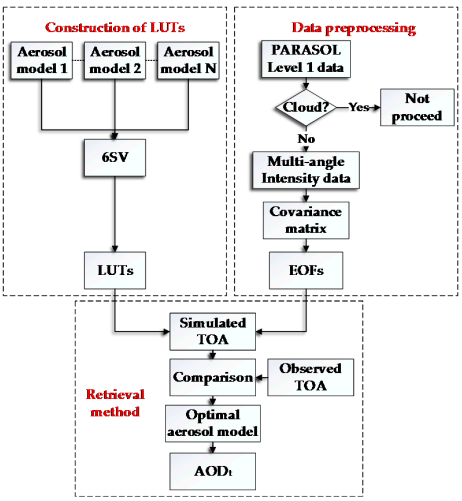

Figure 1. The aerosol optical depth (AOD) retrieval flowchart. LUTs, lookup tables; 6SV, Second Simulation of a Satellite Signal in the Solar Spectrum, Vector version; PARASOL, Polarization and Anisotropy of Reflectances for Atmospheric Science coupled with Observations from a Lidar; EOFs, empirical orthogonal functions; TOA, top of atmosphere.

2.1. A Brief Introduction to the Covariance Matrix

In linear algebra, covariance is defined as

$$cov(X,\ Y) = \frac{\sum_{i=1}^{n}(X_i - \overline{X})(Y_i - \overline{Y})}{n-1} \tag{1}$$

where $cov(X,\ Y)$ is the covariance; X and Y are the sample sets; i is the sample subscript; n is the total number of samples; $\overline{X}$ and $\overline{Y}$ are the means of the sample sets. The covariance matrix is a matrix, the elements of which in the corresponding position are the covariances between two given elements of a random vector. A random vector is a random variable with multiple dimensions. For example, a three-dimensional covariance matrix can be expressed as

$$C = \begin{bmatrix} cov(X,X) & cov(X,Y) & cov(X,Z) \\ cov(Y,X) & cov(Y,Y) & cov(Y,Z) \\ cov(Z,X) & cov(Z,Y) & cov(Z,Z) \end{bmatrix} \tag{2}$$

The covariance matrix is a very important tool in linear algebra and statistics, because every original sample (X_i, Y_i) can be expressed as a linear combination of the eigenvectors of the covariance matrix; these eigenvectors can also be called the EOFs. Remote sensing is an interdisciplinary field that is closely related to linear algebra. Many studies use EOFs to solve concrete questions in remote sensing applications, demonstrating the capability of EOFs. Therefore, the next question is how to use EOFs to estimate the surface contribution in aerosol retrieval.

2.2. The Estimation of Surface Intensity Contribution

The TOA reflectance can be modeled as

$$R_{\lambda}^{TOA}(\mu_s, \mu_v, \varphi) = R_{\lambda}^{atm}(\mu_s, \mu_v, \varphi) + R_{\lambda}^{surf}(\mu_s, \mu_v, \varphi) \tag{3}$$

where $R_{\lambda}^{TOA}(\mu_s, \mu_v, \varphi_s - \varphi_v)$ is the TOA reflectance; λ is the wavelength; μ_s is the cosine of the solar zenith angle; μ_v is the cosine of the view zenith angle; φ is the relative azimuth angle; $R_{\lambda}^{atm}(\mu_s, \mu_v, \varphi)$ is the equivalent reflectance of the atmospheric path radiation; and $R_{\lambda}^{surf}(\mu_s, \mu_v, \varphi)$ is the surface contribution, which is an interaction between the surface and atmosphere.

According to the studies of [12–14], we assume that R_{λ}^{atm} is the same for each pixel in a PARASOL window of 3×3 pixels (19 km); thus, the reduced pixel reflectance for each view geometry in the window can be expressed as

$$J_{x,y} = R_{x,y}^{TOA}(\mu_s, \mu_v, \varphi) - \langle R_{\lambda}^{TOA}(\mu_s, \mu_v, \varphi) \rangle = R_{x,y}^{surf}(\mu_s, \mu_v, \varphi) - \langle R_{\lambda}^{surf}(\mu_s, \mu_v, \varphi) \rangle \tag{4}$$

where $J_{x,y}$ is the reduced reflectance; x, y is the pixel location; and the operation angle brackets denote the average reflectance of the pixels in the window. In fact, $J_{x,y}$ is part of Equation (1), which provides a way to convert the surface contribution to a covariance matrix. In previous studies, this kind of covariance matrix has also been called the "scatter matrix" [18], which can be expressed as

$$C_{ij} = \sum_{x,y} J_{x,y,i} J_{x,y,j} \tag{5}$$

where the subscripts i and j represent the different view angles of PARASOL. The eigenvalues (e_n) and the corresponding eigenvectors (f_n) of the scatter matrix can be solved using linear algebra. As mentioned in Section 2.1, the original sample can be expressed as a linear combination of f_n; thus, the surface contribution of each view angle can be expressed as

$$\langle R_i^{surf} \rangle = \sum_{n=1}^{N_{max}} a_n f_{n,i} \tag{6}$$

where N_{max} is the maximum number of usable eigenvectors, which can be determined by

$$e_{N_{max}} < 2e_{min} < e_{N_{max}-1} \tag{7}$$

where $2e_{min}$ is twice the smallest eigenvalue that presents the noise threshold. Then, the question becomes how to obtain a_n in Equation (6).

As a simple example, we first assume that there is only one bidirectional reflectance factor (BRF) shape in the 3 × 3 window, which means that the pixel surface reflectances are proportional to each other. In this case, the rank of the scatter matrix is one, resulting in a single f_n. Then, the $\langle R_i^{surf} \rangle$ must be proportional to $f_{n,i}$; that is,

$$\langle R_i^{surf} \rangle = a_1 f_{1,i} \tag{8}$$

Combining Equations (3) and (4) yields

$$\langle R_i^{surf} \rangle = \langle R_i^{TOA} \rangle - R_i^{atm} \tag{9}$$

Substituting Equation (8) into Equation (9) for each view angle, we can obtain an equation set as follows:

$$\begin{cases} a_1 f_{1,1} = \langle R_1^{TOA} \rangle - R_1^{atm} \\ a_1 f_{1,2} = \langle R_2^{TOA} \rangle - R_2^{atm} \\ \quad\quad\quad\quad . \\ \quad\quad\quad\quad . \\ \quad\quad\quad\quad . \\ a_1 f_{1,n} = \langle R_n^{TOA} \rangle - R_n^{atm} \end{cases} \tag{10}$$

Multiplying both sides of Equation (10) by the corresponding normalized $f_{1,n}$, and adding up all equations together yields

$$a_1 = \sum_{i=1}^{N_{max}} \left[\langle R_i^{TOA} \rangle - R_i^{atm}(model, \tau) \right] f_{1,i} \tag{11}$$

where model means the aerosol model, and τ is the AOD of the corresponding aerosol model. When more than one BRF shapes exist, Equation (11) can be extended as

$$a_n = \sum_{i=1}^{N_{max}} \left[\langle R_i^{TOA} \rangle - R_i^{atm}(model, \tau) \right] f_{n,i} \tag{12}$$

Thus, the estimation of the surface contribution has been completed. A pivotal feature of this method is the assumption of a uniform atmosphere in a certain area, leaving only surface information in the scatter matrix, which means that the EOFs are completely composed of the surface contribution. Finally, the surface contribution can be obtained by a linear combination of EOFs.

2.3. Retrieval of AOD

In Section 2.2, the surface contribution was obtained, and the next step is to retrieve the AOD. A simple way to obtain AOD is to compare the simulated and observed TOA reflectances for each observation angle. Then, the AOD retrieval is the average of each AOD of the corresponding observation angle that has the minimum simulated residual error. Furthermore, it should be noted that there are various aerosol models for multi-angle aerosol retrievals; therefore, the determination of the optimal aerosol model is indispensable. A basic evaluation method for determining the optimal aerosol model is to calculate the accumulated residual error (η) for each aerosol model, expressed as [19]

$$\eta = \sqrt{\frac{1}{3N_{max}} \sum_{\lambda_0,\lambda_1,\lambda_2} \sum_j \left[R_{sim}^{TOA}(\lambda, \Theta_j) - R_{obs}^{TOA}(\lambda, \Theta_j) \right]^2} \tag{13}$$

where R_{sim}^{TOA} is the simulated TOA reflectance; R_{obs}^{TOA} is the satellite observed TOA reflectance; and λ_0, λ_1, and λ_2 are the 490 nm, 565 nm, and 670 nm PARASOL bands, respectively. The aerosol models with the lowest three η constitute the optimal aerosol models. The concrete aerosol model parameters used in this study can be found in [8] and are presented in Table A1.

3. Results and Validation

3.1. Case Study over East China

Two cases over East China were used to evaluate the performance of our study.

In Figure 2, the Beijing, Tianjing, Hebei, and Liaoning districts are covered by thick grayish aerosols in the true-color image from 21 February 2012. The corresponding AOD retrievals (865 nm) are greater than 0.6, which indicates a case of aerosol pollution. In contrast, the AODs in the Inner Mongolia and Shanxi districts are generally less than 0.1, representing a clean case. For the Henan and Anhui districts, the corresponding AODs are mostly in the range from 0.2 to 0.6, which represents a middle level of pollution. Therefore, Figure 2 shows a complicated aerosol spatial distribution over East China. Figure 3 shows a thin aerosol layer with AODs less than 0.2 in most regions on 23 December 2012. Only a small part of Jiangxi has AODs greater than 0.4, which represents a clean case over a large area of China. The corresponding AERONET ground-based AODs at the Beijing site on 21 February and 23 December 2012 were 0.713 and 0.057, respectively, which suggests that the qualitative determination of AODs for the corresponding regions in our retrieval is correct. The spatial transition of the retrieved AODs in the two figures is smooth, which means that the random error in the retrieval process is small, and suggests the stability of the EOFs in the surface contribution estimation.

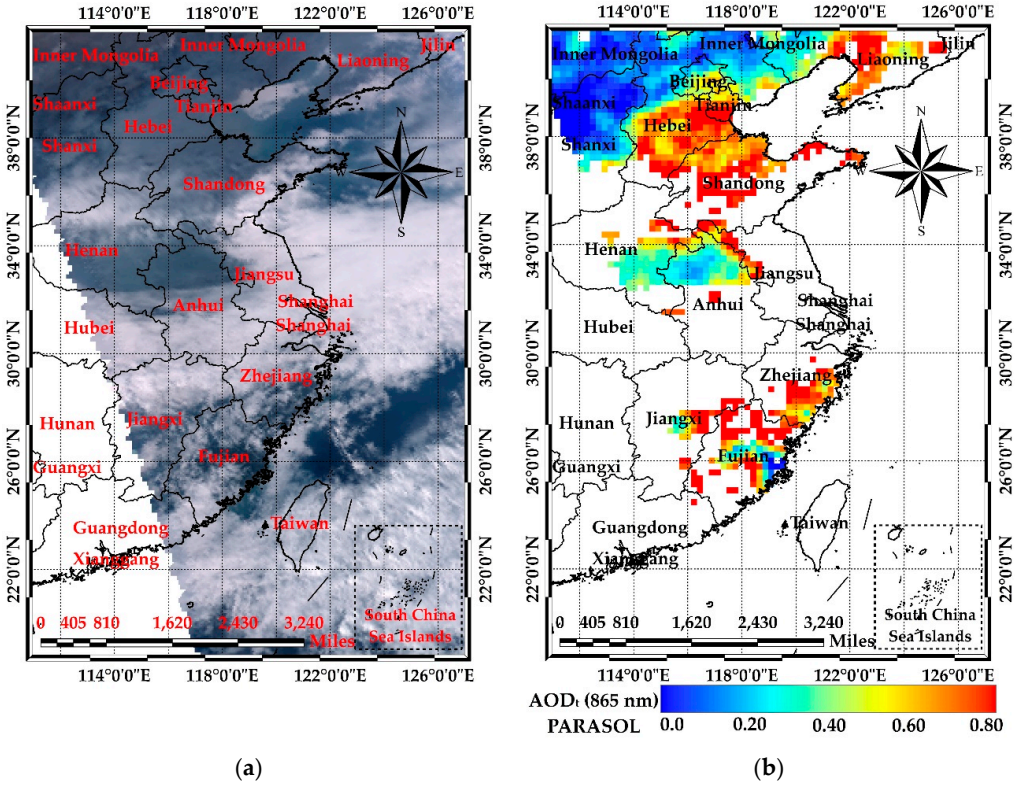

Figure 2. The retrieval results using EOFs from PARASOL; (**a**) is a true-color image for 21 February 2012, (**b**) presents the corresponding AOD retrieval results.

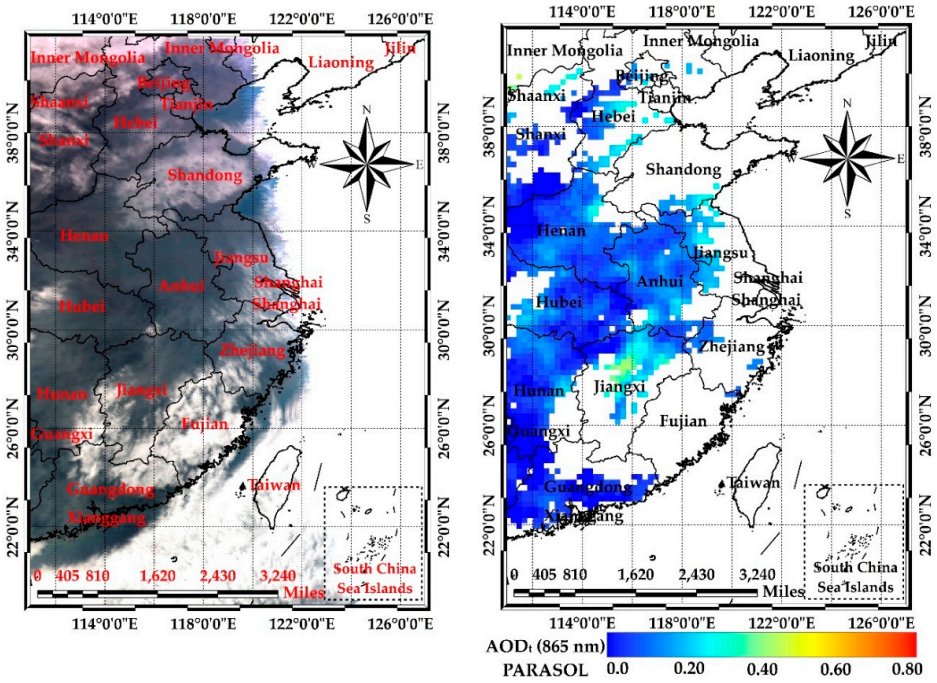

Figure 3. As in Figure 2, but for 23 December 2012.

In conclusion, the above analyses show that the EOF method has applicability for AOD retrieval, at least in a quantitative manner. The quantitative comparison against AERONET ground-based observations is presented in the next section.

3.2. Validation Against AERONET

The AODs over East China from 2011–2013 were retrieved from PARASOL. We chose the ground-based data of four AERONET sites, including Beijing (39.977°N, 116.381°E), Xianghe (39.754°N, 116.962°E), Taihu (31.421°N, 120.215°E), and Hongkong_PolyU (22.303°N, 114.180°E), to validate our retrievals. The AERONET ground-based data for validation are in the Level 2.0 category, with a time threshold of ±60 min between the satellite passes. We used several statistical magnitudes including the correlation coefficient (r), root mean square error (RMSE), mean absolute error (MAE), expected error (EE), and good fraction (Gfrac) to evaluate the retrievals. The RMSE can be expressed as follow:

$$RMSE = \sqrt{\frac{1}{n}\sum_{i=1}^{n}(AOD_{retrieval} - AOD_{AERONET})^2} \quad (14)$$

where $AOD_{retrieval}$ and $AOD_{AERONET}$ are the retrieved and AERONET measured AOD, respectively.

The MAE is calculated as:

$$MAE = \frac{1}{n}\sum_{i=1}^{n}|AOD_{retrieval} - AOD_{AERONET}| \quad (15)$$

The EE [20,21] is defined as:

$$EE = \pm 0.05 \pm 0.15 \times AOD_{AERONET} \quad (16)$$

and the Gfrac represents the fraction of the retrievals falling within EE.

The validation results at the Beijing, Xianghe, Taihu, and Hongkong_PolyU sites are shown in Figure 4. In the figure, the black solid, black dashed, and red solid lines are the 1:1 line, EE envelope line, and fit line, respectively. For Beijing, the r, RMSE, and Gfrac are 0.892, 0.095, and 68.18%, respectively.

For Xianghe, the r, RMSE, and Gfrac are 0.915, 0.093, and 70.51%, respectively. Taihu is often cloudy throughout the year, so there are fewer matched validation points; the corresponding r, RMSE, and Gfrac are 0.831, 0.099, and 72.41%, respectively. The Hongkong_PolyU site is also affected by cloudy weather, leading to fewer matched points; the corresponding r, RMSE, and Gfrac are 0.897, 0.076, and 81.48%, respectively. As a whole, the above validation results show that our retrieval results are in good agreement with those from the AERONET ground-based observations. Table 1 shows that the MAE between the AERONET and the retrieved AOD at the Beijing, Xianghe, Taihu, and Hongkong_PolyU sites are 0.073, 0.074, 0.079, and 0.058, respectively. Along with the corresponding low RMSEs, these values show that our retrievals have good accuracy over the four regions, which also demonstrates that EOFs can be used in quantitative multi-angle aerosol remote sensing estimations for PARASOL observations.

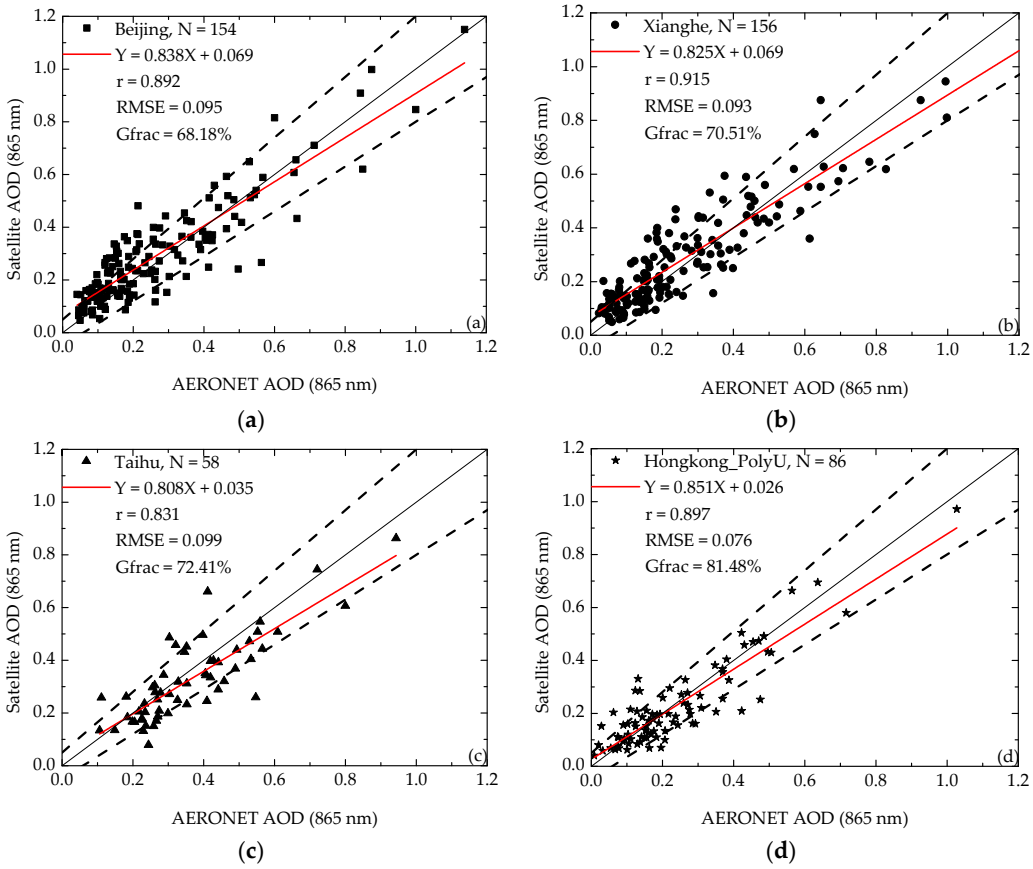

Figure 4. The validation results compared to the Aerosol Robotic Network (AERONET) ground-based observations. (**a**), (**b**), (**c**), and (**d**) are the validation results for the Beijing, Xianghe, Taihu, and Hongkong_PolyU sites, respectively. RMSE, root mean square error; Gfrac, good fraction.

Table 1. Statistical results of the mean AERONET and retrieved AOD (865 nm). MAE, mean absolute error.

AERONET Sites	AERONET AOD Mean	Retrieved AOD Mean	MAE
Beijing	0.260	0.287	0.073
Xianghe	0.264	0.288	0.074
Taihu	0.361	0.328	0.079
Hongkong_PolyU	0.234	0.226	0.058

To evaluate the retrieval accuracy over bright regions, we compared our retrievals with the AERONET ground-based data in the winter (December, January, and February) of 2011–2012 at the Beijing and Xianghe sites, where the retrievals are usually missing in the MODIS DT product during

the same time period. The comparison results are shown in Figure 5. The r, RMSE, MAE, and Gfrac are 0.884, 0.081, 0.063, and 70.09%, respectively, which reveals that our retrievals are comparable with the AERONET ground-based data in winter. This is enough to be of significance, showing that the results make up for the shortage of the MODIS DT product. Although the deep blue (DB) product [22] provides the AOD retrievals over bright regions, the surface reflectivity climatology is required. Our method can accomplish AOD retrieval without any external surface reflectance database.

We also compared the AOD retrievals from the current and previous method at the Beijing and Xianghe sites (Figure 6). Compared with the previous method, the current method achieves an r increase from 0.844 to 0.891, an RMSE decrease from 0.115 to 0.097, an MAE decrease from 0.091 to 0.075, and a Gfrac increase from 57.95% to 69.74%. Moreover, there is no semi-empirical parameter that varies with the study area in our current approach. Therefore, our AOD retrievals represent improvements in both the result and the method.

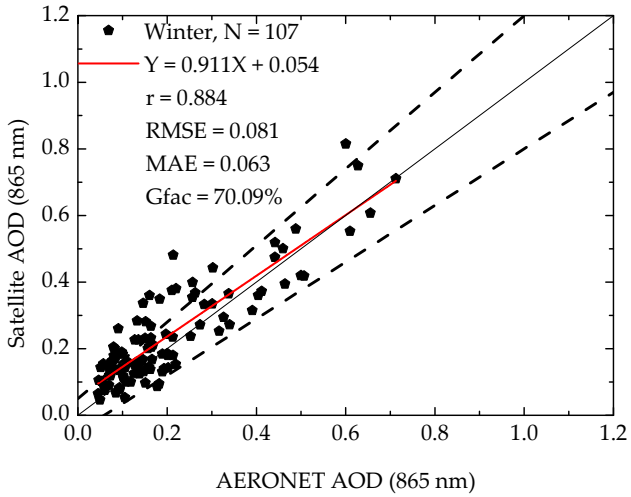

Figure 5. The validation results at the Beijing and Xianghe sites in the winter of 2011–2012.

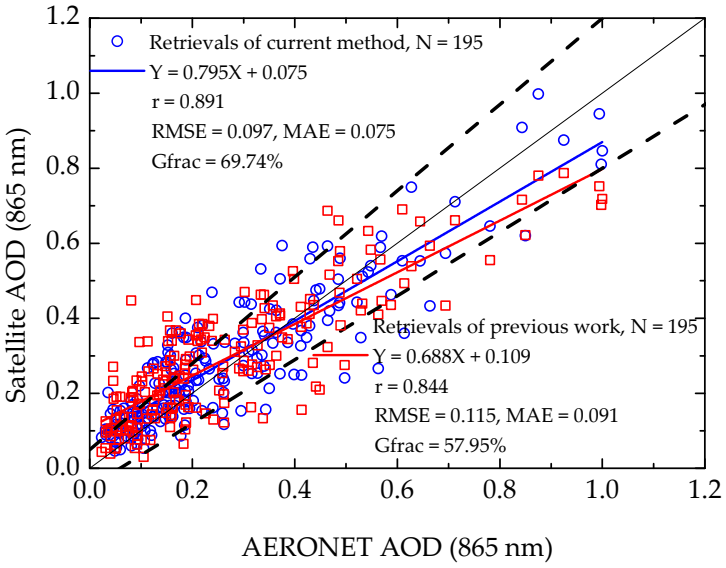

Figure 6. Comparison of results from the current and previous methods at the Beijing and Xianghe sites.

4. Discussion

4.1. EOFs for Surface Contribution Estimation

It should be noted that the Taihu and Hongkong_PolyU sites are located near the water, which means the surface type of the corresponding PARASOL pixels should be a mixture of land and water. The estimation of the surface contribution for these kinds of pixels is generally difficult in the conventional approach. Nevertheless, the validation results for the two sites are good, which indicates a precise surface contribution estimation for the mixed pixels. Therefore, the EOFs are not constrained by the surface type; this means that the surface contribution for any surface type could be obtained by EOFs in theory, and the method does not rely on any semi-empirical parameters, which broadens the scope of applications for this method in aerosol retrieval.

4.2. The Potential of EOFs in Polarized Measurements

From the retrieval and validation results in Section 3, we acknowledge that the EOFs are applicable in the estimation of surface intensity contributions from multi-angle observations. Then, this leads to another question: are EOFs applicable in the estimation of polarized surface contributions? Clearly, there are some differences in the radiative transfer of intensity and polarized lights. A general assumption is that a polarized light mainly comes from single scatterings; however, we think this does not affect the application of EOFs to polarized observations. Regardless of whether the source is from single or multiple scattering, EOFs always calculate the surface contribution, rather than the surface reflectance, which is not affected by the model of the TOA reflectance. We believe that this feature is particularly useful because it resolves the question of the estimation of polarized surface contributions for mixed pixels. The current surface polarized reflectance models generally treat the surface as homogeneous [23–25], which leads to an error in the surface polarized reflectance estimation. Therefore, using EOFs to estimate the surface polarized contribution remains to be addressed in future work.

4.3. The Potential of EOFs in Other Remote Sensing Dimensions

The analysis of remote sensing data can be generalized into five dimensions: spectrum, time, position, angle, and polarization. EOFs were constructed for multi-dimensional data analysis, so they also have the potential to aid in aerosol retrieval across different remote sensing dimensions. In fact, the angle dimension was adopted in both the MISR approach and this study for the retrieval of AOD using EOFs, and this dimension mainly fits a BRF shape. Analogously, if we adopt the spectrum dimension to build the covariance matrix, then it should accordingly produce a description for the shape of the spectral reflectance factor, which could also be applied in aerosol retrieval. Therefore, EOFs are promising for the further development of the aerosol remote sensing field.

4.4. The Limitation of EOFs in Aerosol Retrieval

It should be noticed that the EOF method is based on the covariance matrix, as such, more than one sample is needed to calculate the covariance. Therefore, this method is unable to retrieve the AOD retrieval for a single pixel. The choice of a PARASOL 3×3-pixel window (19 km, which is close to the 17.6 km retrieval window of MISR) in this study is based on previous studies [12–14], indicating that this size could gain an optimized algorithm sensitivity.

5. Conclusions

This paper presented an AOD retrieval method using EOFs to estimate surface intensity contributions based on multi-angle observations from PARASOL, presenting another application example of EOFs for aerosol retrieval in addition to the MISR approach. Two AOD retrievals over East China were performed; the corresponding results show a good qualitative performance of EOFs in

AOD retrieval. The comparisons of the AOD retrievals with AERONET ground-based data produced comparable results for the Beijing, Xianghe, Taihu, and Hongkong_PolyU sites, with corresponding r values of 0.892, 0.915, 0.831, and 0.897, respectively, and MAE values of 0.073, 0.074, 0.079, and 0.058, respectively, revealing that EOFs are practical and useful in the quantitative retrieval of AOD from the PARASOL multi-angle intensity data. Furthermore, EOFs can retrieve the AOD over bright regions; the retrievals for the Beijing and Xianghe sites in winter are in good agreement with the AERONET ground-based data. Compared with our previous approach, the AOD retrievals also exhibited an accuracy improvement, and no semi-empirical parameter is required in our current approach. Although it is difficult to use EOFs to achieve the aerosol retrieval for a single pixel, which leads to the spatial resolution of 19 km of our result, it could still meet most requirements in atmospheric and environmental applications.

EOFs are useful mathematical tools for multi-dimensional data analysis, in addition to the analysis of the multi-angle information used in this study. Many other observation dimensions can be employed to build the covariance matrix, which is a very promising prospect in aerosol retrieval. Therefore, the application of EOFs in aerosol retrieval needs further study. We plan to conduct future research on retrieval from the spectral and polarized dimensions.

Acknowledgments: This work was supported by the National Natural Science Foundation of China (Grant No. 41671367, No. 41671364, No. 41601385, No. 41505022, No.41501399), the Instrument Developing Project of the Chinese Academy of Sciences (Grant No. YZ201664), the Major Project of High Resolution Earth Observation System (Grant No.: 30-Y20A39-9003-15/17). We thank Hongbin Chen, Philippe Goloub, Pucai Wang, Xiangao Xia, Ronghua Ma, and Janet Elizabeth Nichol for their efforts in establishing and maintaining the Beijing, Xinglong, Xianghe, Taihu, and Hong_Kong_PolyU AERONET sites. We thank the ICARE Data and Services Center for providing access to the data used in this study. We thank Eric F. Vermote, Jean-Claude Roger, S.Y. Kotchenova, J.J. Morcrette, D. Tanré, J.L. Deuzé, and M. Herman for the 6SV Radiative Transfer code. We sincerely thank American Journal Experts (AJE) for their helpful English language editing. Finally, we sincerely thank the anonymous reviewers for their helpful comments. We are additionally thankful for the full technical edit provided by one of the anonymous reviewers.

Author Contributions: All authors conceived and designed the study. Yang Zhang and Zhengqiang Li performed the AOD retrieval using EOFs and prepared the paper. Lili Qie provided useful advice regarding the programming realization of EOFs. Weizhen Hou and Zhihong Liu provided technical guidance and revised the paper. Yisong Xie and Xingfeng Chen assisted with the data preprocessing. Ying Zhang and Hua Xu assisted with the satellite and ground-based data collection.

Conflicts of Interest: The authors declare no conflict of interest.

Appendix A

The aerosol size follows a log-normal distribution, defined as

$$\frac{dN}{dr} = \frac{N_0}{\sqrt{2\pi}\sigma_n} exp\left[-\frac{(lnr - lnr_n)^2}{2{\sigma_n}^2}\right] \tag{A1}$$

where N_0 is the number of particles per cross section of the atmospheric column, r_n is the modal radius, and σ_n is the standard deviation of lnr_n. We assume that the size distribution has two modes. The model parameters are shown in Table A1.

Table A1. The parameters for the aerosol models used in this study [8,26,27]. m_r is the real part of the complex refractive index, m_i is the imaginary part of the complex refractive index, Fine and Coarse refer to the fine- and coarse-mode, respectively, and C is the percentage density of fine particles by number.

Class	Parameters						
	m_r	m_i	$r_{n,\ Fine}$	$\sigma_{n,\ Fine}$	$r_{n,\ Coarse}$	$\sigma_{n,\ Coarse}$	C
1	1.483	0.0078	0.1089	0.535	0.9801	0.568	0.05
2	1.5465	0.0130	0.1202	0.6135	0.9724	0.6022	0.13
3	1.485	0.0088	0.0939	0.531	0.9826	0.583	0.20
4	1.537	0.0023	0.0659	0.619	0.9618	0.531	0.43
5	1.5393	0.0129	0.0845	0.6157	0.8287	0.6126	0.53
6	1.528	0.0148	0.0839	0.5406	0.7476	0.6281	0.60
7	1.468	0.0102	0.0896	0.504	0.9269	0.618	0.76
8	1.482	0.009	0.0902	0.474	0.6229	0.656	0.82
9	1.4853	0.0095	0.095	0.5246	0.7958	0.6451	0.90
10	1.5465	0.013	0.1202	0.6135	0.9724	0.6022	0.99

References

1. Nicolas, B.; Olivier, B.; Jim, H.; Shekar, R.M. Global estimate of aerosol direct radiative forcing from satellite measurements. *Nature* **2006**, *438*, 1138–1141.
2. Liu, Y.; Franklin, M.; Kahn, R.; Koutrakis, P. Using aerosol optical thickness to predict ground-level $PM_{2.5}$ concentrations in the St. Louis area: A comparison between misr and modis. *Remote Sens. Environ.* **2007**, *107*, 33–44. [CrossRef]
3. Schwartz, C.S.; Liu, Z.; Lin, H.C.; Mckeen, S.A. Simultaneous three-dimensional variational assimilation of surface fine particulate matter and modis aerosol optical depth. *J. Geophys. Res.* **2012**, *117*, 110–117. [CrossRef]
4. Puttaswamy, S.J.; Hai, M.N.; Braverman, A.; Hu, X.; Liu, Y. Statistical data fusion of multi-sensor aod over the continental united states. *Geocarto Int.* **2013**, *29*, 48–64. [CrossRef]
5. Schwartz, C.S.; Liu, Z.; Lin, H.C.; Cetola, J.D. Assimilating aerosol observations with a "hybrid" variational-ensemble data assimilation system. *J. Geophys. Res. Atmos.* **2014**, *119*, 4043–4069. [CrossRef]
6. Zhang, Y.; Li, Z. Remote sensing of atmospheric fine particulate matter ($PM_{2.5}$) mass concentration near the ground from satellite observation. *Remote Sens. Environ.* **2015**, *160*, 252–262. [CrossRef]
7. Li, Z.; Zhang, Y.; Shao, J.; Li, B.; Hong, J.; Liu, D.; Li, D.; Wei, P.; Li, W.; Li, L.; et al. Remote sensing of atmospheric particulate mass of dry $PM_{2.5}$ near the ground: Method validation using ground-based measurements. *Remote Sens. Environ.* **2016**, *173*, 59–68. [CrossRef]
8. Zhang, Y.; Li, Z.; Qie, L.; Zhang, Y.; Liu, Z.; Chen, X.; Hou, W.; Li, K.; Li, D.; Xu, H. Retrieval of aerosol fine-mode fraction from intensity and polarization measurements by parasol over east asia. *Remote Sens.* **2016**, *8*, 417. [CrossRef]
9. Von Hoyningen-Huene, W. Retrieval of aerosol optical thickness over land surfaces from top-of-atmosphere radiance. *J. Geophys. Res.* **2003**, *108*, D9. [CrossRef]
10. Kaufman, Y.J.; Wald, A.E.; Remer, L.A.; Gao, B.C. The modis 2.1-μm channel-correlation with visible reflectance for use in remote sensing of aerosol. *IEEE Trans. Geosci. Remote Sens.* **1997**, *35*, 1286–1298. [CrossRef]
11. Levy, R.C.; Remer, L.A.; Mattoo, S.; Vermote, E.F.; Kaufman, Y.J. The second-generation operational algorithm: Retrieval of aerosol properties over land from inversion of modis spectral reflectance. *J. Geophys. Res.* **2007**, *112*, D13211. [CrossRef]
12. Martonchik, J.V. Determination of aerosol optical depth and land surface directional reflectances using multiangle imagery. *J. Geophys. Res. Atmos.* **1997**, *102*, 17015–17022. [CrossRef]
13. Martonchik, J.V.; Diner, D.J.; Kahn, R.A.; Ackerman, T.P.; Verstraete, M.M.; Pinty, B.; Gordon, H.R. Techniques for the retrieval of aerosol properties over land and ocean using multi-angle imaging. *IEEE Trans. Geosci. Remote Sens.* **1998**, *36*, 1212–1227. [CrossRef]

14. Diner, D.J.; Martonchik, J.V.; Kahn, R.A.; Pinty, B.; Gobron, N.; Nelson, D.L.; Holben, B.N. Using angular and spectral shape similarity constraints to improve misr aerosol and surface retrievals over land. *Remote Sens. Environ.* **2005**, *94*, 155–171. [CrossRef]
15. Vermote, E.F.; Tanré, D.; Deuzé, J.L.; Herman, M.; Morcette, J.J. Second simulation of the satellite signal in the solar spectrum, 6s: An overview. *IEEE Trans. Geosci. Remote Sens.* **1997**, *35*, 675–686. [CrossRef]
16. Kotchenova, S.Y.; Vermote, E.F.; Raffaella, M.; Klemm, F.J. Validation of a vector version of the 6s radiative transfer code for atmospheric correction of satellite data. Part I: Path radiance. *Appl. Opt.* **2006**, *45*, 6762–6774. [CrossRef] [PubMed]
17. Kotchenova, S.Y.; Vermote, E.F. Validation of a vector version of the 6s radiative transfer code for atmospheric correction of satellite data. Part II: Homogeneous lambertian and anisotropic surfaces. *Appl. Opt.* **2007**, *46*, 6762–6774. [CrossRef]
18. Preisendorfer, R.W.; Mobley, C.D. Principal component analysis in meteorology and oceanography. *Dev. Atmos. Sci.* **1988**, *17*, 55–72.
19. Deuzé, J.L.; Bréon, F.M.; Devaux, C.; Goloub, P.; Herman, M.; Lafrance, B.; Maignan, F.; Marchand, A.; Nadal, F.; Perry, G.; et al. Remote sensing of aerosols over land surfaces from polder-adeos-1 polarized measurements. *J. Geophys. Res.* **2001**, *106*, 4913. [CrossRef]
20. Chu, D.A.; Kaufman, Y.J.; Ichoku, C.; Remer, L.A.; Tanré, D.; Holben, B.N. Validation of modis aerosol optical depth retrieval over land. *Geophys. Res. Lett.* **2002**, *29*, 8007. [CrossRef]
21. Levy, R.C.; Remer, L.A.; Kleidman, R.G.; Mattoo, S. Global evaluation of the collection 5 modis dark-target aerosol products over land. *Atmos. Chem. Phys.* **2010**, *10*, 10399–10420. [CrossRef]
22. Hsu, N.C.; Tsay, S.C.; King, M.D.; Herman, J.R. Aerosol properties over bright-reflecting source regions. *IEEE Trans. Geosci. Remote Sens.* **2004**, *42*, 557–569. [CrossRef]
23. Nadal, F.; Breon, F.M. Parameterization of surface polarized reflectance derived from polder spaceborne measurements. *IEEE Trans. Geosci. Remote Sens.* **1999**, *37*, 1709–1718. [CrossRef]
24. Maignan, F.; Bréon, F.-M.; Fédèle, E.; Bouvier, M. Polarized reflectances of natural surfaces: Spaceborne measurements and analytical modeling. *Remote Sens. Environ.* **2009**, *113*, 2642–2650. [CrossRef]
25. Xie, D.; Cheng, T.; Wu, Y.; Fu, H.; Zhong, R.; Yu, J. Polarized reflectances of urban areas: Analysis and models. *Remote Sens. Environ.* **2017**, *193*, 29–37. [CrossRef]
26. Lee, K.H.; Kim, Y.J. Satellite remote sensing of asian aerosols: A case study of clean, polluted, and asian dust storm days. *Atmos. Meas. Tech.* **2010**, *3*, 1771–1784. [CrossRef]
27. Li, S.; Chen, L.; Tao, J.; Han, D.; Wang, Z.; Su, L.; Fan, M.; Yu, C. Retrieval of aerosol optical depth over bright targets in the urban areas of north china during winter. *Sci. China Earth Sci.* **2012**, *55*, 1545–1553. [CrossRef]